Mueller matrix dual-rotating retarder polarimeter

Dennis H. Goldstein

A computer-controlled Mueller matrix polarimeter with dual rotating retarders is described. Bulk properties of optical materials are determined by controlling the input-polarization state and measuring the output-polarization state. The Mueller matrix of a sample is obtained from polarimetric measurements, and polarization properties, i.e., diattenuation and retardance as well as depolarization, are extracted from the Mueller matrix. Further, fundamental electro- and magneto-optical material properties such as the electro-optical tensor coefficients may be obtained from Mueller matrices measured with applied fields. The polarimeter is currently configured to operate over the 3- to 12-μm spectral region.

Key words: Mueller matrix, polarimetry, laser polarimetry, ellipsometry.

1. Introduction

Polarimetry is an experimental technique for measuring the polarization state of a light beam and for deducing the polarizing properties of bulk materials in transmission. (Azzam and Bashara refer to this as "transmission ellipsometry" in their treatise on ellipsometry.[1]) A polarimeter is an optical instrument used for the determination of the polarization state of a light beam.

Polarimeters are commonly used to measure specific optical properties of media in diverse applications.[2–9] The most general information that can be obtained from a polarimeter is the Mueller matrix, a 4×4 real matrix that contains all information concerning the polarization properties of a medium except the overall phase. (Overall phase information, as measured in interferometry, is lost in Mueller matrix polarimetry. Relative phase information between polarization states, or retardance, is determined.)

I have constructed a Mueller matrix polarimeter based on an ellipsometric method proposed by Azzam.[10] My purpose in constructing and operating this instrument is to determine properties such as retardance, diattenuation, and depolarization of linear or nonlinear electro- and magneto-optic materials in the infrared region of the spectrum. The polarimeter radiation source is currently a tunable CO_2 laser.

The author is with the U.S. Air Force Wright Laboratory Armament Directorate, WL/MNGS, Eglin Air Force Base, Florida 32542-5434.

Received 13 May 1991.

2. Infrared Mueller Matrix Rotating-Retarder Polarimeter

The infrared laser polarimeter described here is designed for operation with any laser source in the 3- to 12-μm spectral region. This spectral region is of great interest for the evaluation of materials used as elements of optical-processing systems, laser-modulation systems, or thermal-imaging systems. The polarimeter design is readily adapted for operation in other wavelength regions with different sources, detectors, and elements.

This polarimeter configuration is based on designs described by Azzam[10] and by Hauge.[11] The technique has been used with the sample in reflection to measure birefringence in the human eye at visible wavelengths.[12–14] Mueller matrix elements and Stokes vectors are used to represent the polarization elements and polarized light, respectively. The Mueller matrix formulation is used over the Jones formulation because it is preferable for experimental research where scattering and depolarization measurements are made routinely.

Figure 1 shows a functional block diagram of the polarimeter. The polarimeter has five sections: the laser source, the polarizing optics, the sample, the analyzing optics, and the detector.

The polarizing optics consist of a fixed linear polarizer and a quarter-wave plate that rotates. The sample region is followed by the analyzing optics, which consist of a quarter-wave plate that rotates followed by a fixed linear polarizer. One of the great advantages of this configuration is that the polarization sensitivity of the detector is not important because the orientation of the final polarizer is fixed.

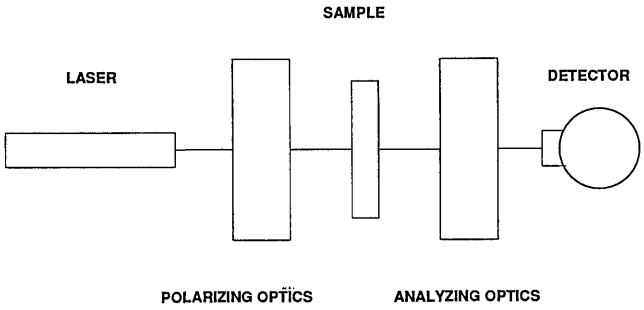

Fig. 1. Polarimeter block diagram. The Mueller matrix of the sample is determined from the modulated intensity measured by the detector.

The two wave plates are rotated at different but harmonic rates, and a modulation of the detected intensity results. The Mueller matrix of the sample is found through a relationship between the Fourier coefficients of a series representing the modulation and the elements of the sample matrix.

Figure 2 shows a diagram of the instrument in its actual implementation. The source beam is chopped at ~1 kHz because the detector electronics require a modulated signal. A beam splitter diverts a fraction of the beam to monitor the laser output power. The main beam passes through the polarimeter elements, the sample, and on to the detector. A preamplifier provides a bias voltage to the detector and an output voltage for a multimeter. The detector is used in its linear region.

The polarizer P2 is an infrared wire grid polarizer. The polarization of the laser, which is linearly polarized, provides the initial polarization of the beam so that no linear polarizer is needed before the sample. All other polarization elements are aligned relative to the laser polarization. This dual-rotating retarder-polarimeter technique requires a rotating linear retarder on both sides of the sample to modulate the various Mueller matrix elements onto intensity variations in separate modulation frequencies. The retarders R1 and R2 used with the CO_2 laser are cadmium sulfide zero-order wave plates, giving nominally a 90° phase shift between orthogonal polarization states at 10.6 μm. (Wave plates with almost any retardation values may be used; however, the intensity modulation that results with quarter-wave plates contains null points, i.e., there is greater

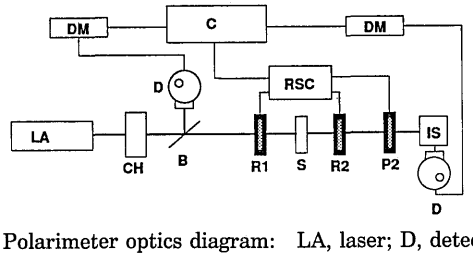

Fig. 2. Polarimeter optics diagram: LA, laser; D, detector; PZ, polarizer; R1, R2, retarders; S, sample; CH, chopper; IS, integrating sphere; B, beam splitter; C, computer; RSC, rotary stage controller; DM, digital multimeter.

modulation.) Actual values of the retardance (supplied by the manufacturer) for the retarders used here were slightly different from 90°. The compensation for nonideal wave plates is discussed later and is one of the unique features of this instrument.

The final elements in the sample measurement leg are a small infrared integrating sphere and a HgCdTe photoconductive detector with a low-noise preamplifier. The photoconductive detector preamplifier is powered by a dc power supply. The integrating sphere serves as the radiation collector. HgCdTe detectors are currently not available in large sizes (>4 mm on a side). To collect all radiation in a larger beam, or to eliminate a beam wander caused by deviation of the beam from a rotating element with nonparallel faces, one must have a larger detector area. This larger area is effectively obtained by using the integrating sphere as a collector. A small infrared integrating sphere of 5.08 cm diameter has a collecting aperture of 1.27 cm. A HgCdTe detector is then placed in the detector port of the integrating sphere.

All three polarizing elements are held in motorized rotary stages connected to a programmable stage controller. The controller is in turn connected to a computer by means of an IEEE-488 bus. The rotary stages are driven with dc motors and have optical encoders with resolution control to .001°.

The detector preamplifier outputs are connected to digital multimeters, which are in turn connected to the computer by means of the IEEE −488 bus. The central computer controls the orientation of the polarizing elements and monitors the data arriving from the detectors. Data are displayed on the computer screen or output to a printer and plotter. All the software necessary for calibration procedures, data acquisition, and preliminary processing is stored on this computer.

The computer is programmed in BASIC to rotate the wave plates and query the multimeters. The second wave plate is rotated five times the rate of the first, and data are typically collected for every 2 to 6° of rotation of the first wave plate. The stages are stopped completely after each incremental rotation, and an intensity reading is recorded. The resulting data set is a modulated waveform, which is then processed according to the algorithms in Section 3.

The three polarizing elements in the polarimeter are required to be aligned with respect to the laser-polarization axis orientation to within a small angle (of the order of 0.1°). The principal objective of the polarimeter calibration is to orient the linear polarizer so that its axis is parallel with the laser-polarization axis and then to orient the retarders so that their fast axes are parallel with each other and parallel with the polarizer axis. This process is the subject of considerable effort, and the elimination of the remaining errors form a substantial part of this research, as summarized in Section 4.

3. Mathematical Development: Obtaining the Mueller Matrix

This polarimeter measures a chopped signal, which is modulated by rotating the polarizing optical elements. The elements of the Mueller matrix are encoded on the modulated signal. The output signal is then Fourier analyzed to determine the Mueller matrix elements. The implementation described here uses two aligned and fixed linear polarizers and two rotating quarter-wave retarders as shown in Fig. 3. The second retarder is rotated at a rate of five times that of the first. This generates twelve harmonic frequencies in the Fourier spectrum of the modulated intensity.

The following treatment through Eq. (9) is based on a derivation by Azzam.[10] The Mueller matrix for the system is

$$\mathbf{P}_2\mathbf{R}_2(\theta)\mathbf{M}\mathbf{R}_1(\theta)\mathbf{P}_1, \tag{1}$$

where $\mathbf{P}$ indicates a linear polarizer, $\mathbf{R}(\theta)$ indicates an orientation-dependent linear retarder, and $\mathbf{M}$ is the sample and is the matrix quantity to be determined. Mueller matrices are then substituted for a linear retarder with quarter-wave retardation and a fast axis at θ and 5θ for $\mathbf{R}_1$ and $\mathbf{R}_2$, respectively; a horizontal linear polarizer for $\mathbf{P}_2$; a horizontal linear polarizer for $\mathbf{P}_1$ (in practice, the need for this polarizer is eliminated because a highly polarized laser is used as the source); and a sample for $\mathbf{M}$. The Mueller matrices for the optical elements are tabulated in various references as functions of retardation and orientation angles.[15,16] The detected intensity is given by

$$I = c\mathbf{AMP}, \tag{2}$$

where $\mathbf{P} = \mathbf{R}_1\mathbf{P}_1\mathbf{S}$ is the Stokes vector of light leaving the polarizing optics ($\mathbf{S}$ is the Stokes vector of the light from the source), $\mathbf{A} = \mathbf{P}_2\mathbf{R}_2$ is the Mueller matrix of the analyzing optics, $\mathbf{M}$ is the Mueller matrix of the sample, and c is a proportionality constant obtained from the absolute intensity. Explicitly,

$$I = c\sum_{i,j=1}^{4} a_i p_j m_{ij}, \tag{3}$$

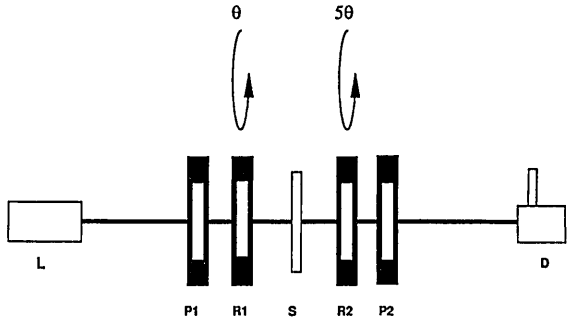

Fig. 3. Polarizing elements and rotation rates. A laser source L is directed through fixed polarizers P1 and P2, rotating retarders R1 and R2, and the sample S, to a detector.

or

$$I = c\sum_{i,j=1}^{4} \mu_{ij} m_{ij}, \tag{4}$$

where the a_i are the elements of the first row of $\mathbf{A}$, the p_j are the elements of $\mathbf{P}$, the m_{ij} are the elements of the Mueller matrix $\mathbf{M}$, and where

$$\mu_{ij} = a_i p_j. \tag{5}$$

The order of matrix multiplication can be changed as shown above in going from Eq. (2) to Eq. (3) because we are only measuring the intensity, i.e., the first element of the Stokes vector. Only the first row of the matrix $\mathbf{A}$ is involved in the calculation:

$$\begin{bmatrix} a_1 & a_2 & a_3 & a_4 \\ \cdot & \cdot & \cdot & \cdot \\ \cdot & \cdot & \cdot & \cdot \\ \cdot & \cdot & \cdot & \cdot \end{bmatrix} \begin{bmatrix} m_{11} & m_{12} & m_{13} & m_{14} \\ m_{21} & m_{22} & m_{23} & m_{24} \\ m_{31} & m_{32} & m_{33} & m_{34} \\ m_{41} & m_{42} & m_{43} & m_{44} \end{bmatrix} \begin{bmatrix} p_1 \\ p_2 \\ p_3 \\ p_4 \end{bmatrix} = \begin{bmatrix} I \\ \cdot \\ \cdot \\ \cdot \end{bmatrix}, \tag{6}$$

and multiplying through

$$\begin{aligned} I = {} & a_1(m_{11}p_1 + m_{12}p_2 + m_{13}p_3 + m_{14}p_4) \\ & + a_2(m_{21}p_1 + m_{22}p_2 + m_{23}p_3 + m_{24}p_4) \\ & + a_3(m_{31}p_1 + m_{32}p_2 + m_{33}p_3 + m_{34}p_4) \\ & + a_4(m_{41}p_1 + m_{42}p_2 + m_{43}p_3 + m_{44}p_4) \\ = {} & \sum_{i,j=1}^{4} \mu_{ij} m_{ij}. \end{aligned} \tag{7}$$

When the rotation ratio is 5:1 the μ_{ij} are given by

$$\begin{aligned} \mu_{11} &= 1, \\ \mu_{12} &= \cos^2 2\theta, \\ \mu_{13} &= \sin 2\theta \cos 2\theta, \\ \mu_{14} &= \sin 2\theta, \\ \mu_{21} &= \cos^2 10\theta, \\ \mu_{22} &= \cos^2 2\theta \cos^2 10\theta, \\ \mu_{23} &= \sin 2\theta \cos 2\theta \cos^2 10\theta, \\ \mu_{24} &= \sin 2\theta \cos^2 10\theta, \\ \mu_{31} &= \sin 10\theta \cos 10\theta, \\ \mu_{32} &= \cos^2 2\theta \sin 10\theta \cos 10\theta, \\ \mu_{33} &= \sin 2\theta \cos 2\theta \sin 10\theta \cos 10\theta, \\ \mu_{34} &= \sin 2\theta \sin 10\theta \cos 10\theta, \\ \mu_{41} &= -\sin 10\theta, \\ \mu_{42} &= -\cos^2 2\theta \sin 10\theta, \\ \mu_{43} &= -\sin 2\theta \cos 2\theta \sin 10\theta, \\ \mu_{44} &= -\sin 2\theta \sin 10\theta. \end{aligned} \tag{8}$$

These equations can be expanded in a Fourier series to yield the Fourier coefficients, which are functions of the Mueller matrix elements.

The inversion of these relations gives the Mueller matrix elements in terms of the Fourier coefficients:

$$
\begin{aligned}
m_{11} &= a_0 - a_2 + a_8 - a_{10} + a_{12},\\
m_{12} &= 2a_2 - 2a_8 - 2a_{12},\\
m_{13} &= 2b_2 + 2b_8 - 2b_{12},\\
m_{14} &= b_1 - 2b_{11} = b_1 + 2b_9 = b_1 + b_9 - b_{11},\\
m_{21} &= -2a_8 + 2a_{10} - 2a_{12},\\
m_{22} &= 4a_8 + 4a_{12},\\
m_{23} &= -4b_8 + 4b_{12},\\
m_{24} &= -4b_9 = 4b_{11} = 2(-b_9 + b_{11}),\\
m_{31} &= -2b_8 + 2b_{10} - 2b_{12},\\
m_{32} &= 4b_8 + 4b_{12},\\
m_{33} &= 4a_8 - 4a_{12},\\
m_{34} &= 4a_9 = -4a_{11} = 2(a_9 - a_{11}),\\
m_{41} &= 2b_3 - b_5 = -b_5 + 2b_7 = (b_3 - b_5 + b_7),\\
m_{42} &= -4b_3 = -4b_7 = -2(b_3 + b_7),\\
m_{43} &= -4a_3 = 4a_7 = 2(-a_3 + a_7),\\
m_{44} &= -2a_4 = 2a_6 = (a_6 - a_4).
\end{aligned}
\tag{9}
$$

The 5:1 rotation ratio is not the only ratio that can be used to determine Mueller matrix elements, but it is the lowest ratio in which the expressions for the Fourier coefficients may be inverted to give the Mueller matrix elements.

Intensity values in the form of voltages are measured as the retarders are incrementally advanced such that the first retarder rotates through 180°. The Fourier coefficients must be obtained from the measured intensity values. There are several methods of formulating the solution to this problem.

If the problem is formulated as

$$xa = I, \tag{10}$$

where I is a vector of 36 intensity values, a is the set of 25 Fourier coefficients, and x is a 36 × 25 matrix where each row is of the form

$$(1 \cos 2\theta \cos 4\theta \ldots \cos 24\theta \sin 2\theta \sin 4\theta \ldots \sin 24\theta)$$

where the θ for each row represents the angle of the fast axis of the first retarder, then the solution is

$$a = (x^T x)^{-1} x^T I. \tag{11}$$

(The minimum number of equations needed to solve for the coefficients uniquely is 25 so that the maximum rotational increment for the first retarder is 7.2°; for this example, 36 equations are obtained from 5° rotational increments through 180°.) This solution is equivalent to the least-squares solution.[17] In the least-squares formulation the expression for the instrument response is

$$I(\theta) = a_o + \sum_{j=1}^{12} (a_j \cos 2j\theta + b_j \sin 2j\theta), \tag{12}$$

but the actual measurement $\Phi(\theta)$ may be different than this value. The sum of the square of these differences may be formed, i.e.,

$$\sum_{l=0}^{35} [\Phi(\theta_l) - I(\theta_l)]^2 = E(a_0, a_1, \ldots, a_{12}, b_1, \ldots, b_{12}), \tag{13}$$

where E is a function of the coefficients and l is the subscript of the retarder angle. The values of the coefficients can now be found by taking the partial derivative of E with respect to the coefficients and setting these equal to zero:

$$\frac{\delta E}{\delta a_k} = 0, \qquad \frac{\delta E}{\delta b_k} = 0. \tag{14}$$

The expression becomes, for the derivative with respect to a_l,

$$\sum_{l=0}^{35} \left\{ \Phi(\theta_l) - \left[a_0 + \sum_{j=1}^{12} (a_j \cos 2j\theta_l + b_j \sin 2j\theta_l \right] \right\} \times (-2 \cos 2k\theta_l) = 0. \tag{15}$$

Solving this system of 36 equations in 25 unknowns will give the least-squares solution for the coefficients, which is identical to the solution obtained from Eq. (11).

4. Error Compensation

The true nature of the sample may be obscured by errors inherent in the polarimeter optical system. The Mueller matrix elements must be compensated for the known errors in retardance of the retarders and the errors caused by the inability to align the polarizing elements precisely. The fact that there are errors that cannot be eliminated through optical means led to an error analysis and a compensation procedure to be implemented during polarimeter data processing.

A summary of an error analysis of a dual-rotating retarder Mueller matrix polarimeter is presented in this section. The derivation of the compensated Mueller matrix elements using the small-angle approximation is documented in detail in Goldstein and Chipman.[18] Errors in orientational alignment are considered. Errors caused by nonideal retardation elements are also included in the analysis. A compensation for imperfect retardation elements is then made possible with the equations derived, and the equations permit a calibration of the polarimeter for the azimuthal alignment of the polarization elements.

A similar analysis was done by Hauge[11] for a dual-rotating compensator ellipsometer, but this analysis did not include error in the last polarizer and did include errors caused by diattenuation in the retardation elements. Experimental experience with the polarimeter described here indicates that the deviation of the retarders from the quarter wave is important compared with the diattenuation of the retarders.

In the error analysis, the effect of retardation associated with the polarizers and polarization associated with the retarders have not been included. It is also assumed that there are no angular errors associated with the stages that rotate the elements. It is only the relative orientations of the polarizers and retarders that are relevant, and the analysis is simplified by measuring all angles relative to the angle of the laser polarization. The three polarization elements have errors associated with their initial azimuthal alignment with respect to the laser polarization. In addition, one or both retarders may have retardances that differ from a quarter wave. In general, both retarders will have different retardances and the three polarization elements will be slightly misaligned in azimuth. Figure 4 illustrates these errors.

Exact expressions for compensated Fourier coefficients are derived in Ref. 18. Because the error angles are typically small, the Fourier coefficients can be expressed by using small-angle approximations. The expressions for the Fourier coefficients given below in Eq. (16) reflect this small-angle approximation.

The following calibration procedure is used. First, the polarimeter is operated with no sample and Fourier coefficients obtained from the measured modulated intensity. Second, using error-compensation equations with matrix elements of the identity matrix inserted for the Mueller matrix elements, I calculate the errors in the element orientations and retardances. Third, in the routine use of the polarimeter, the systematic errors in the Fourier coefficients arising from the imperfections are compensated for by using the error-compensated equations with experimentally determined error values to obtain the error-compensated sample Mueller matrix elements as a function of measured Fourier coefficients.

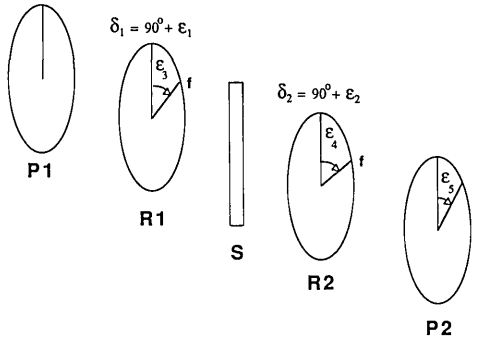

Fig. 4. Retardation errors ϵ_1 and ϵ_2, and orientation errors ϵ_3, ϵ_4, and ϵ_5: P1, P2, fixed polarizers; R1, R2, rotating retarders; S, sample; f, fast axis.

With no sample in the polarimeter, the sample matrix is the identity matrix. Because all off-diagonal elements in the sample Mueller matrix are zero, all odd Fourier coefficients in Eq. (12) become zero. Because the diagonal elements equal one, the coefficients of the twelfth harmonic vanish also. The fourth and sixth Fourier cosine coefficients are useless for determining errors because they are not functions of the error. The Fourier coefficients a_0, a_2, a_8, a_{10}, b_2, b_4, b_6, b_8, and b_{10} are functions of the errors as follows:

$$
\begin{aligned}
a_0 &= \frac{1}{4} + \frac{(1-\epsilon_1)(1-\epsilon_2)}{16}, \\
a_2 &= \frac{(1+\epsilon_1)(1-\epsilon_2)}{16} + \frac{(1+\epsilon_1)(1-\epsilon_2)\epsilon_3\epsilon_5}{2}, \\
a_8 &= \frac{(1+\epsilon_1)(1+\epsilon_2)}{16}, \\
a_{10} &= \frac{(1-\epsilon_1)(1+\epsilon_2)}{16}, \\
b_2 &= -\frac{(1+\epsilon_1)(1-\epsilon_2)\epsilon_3}{4} + \frac{(1+\epsilon_1)(1-\epsilon_2)\epsilon_5}{8}, \\
b_4 &= \frac{(\epsilon_4 - \epsilon_3 - \epsilon_5)}{4}, \\
b_6 &= \frac{(\epsilon_5 - \epsilon_3 - \epsilon_4)}{4}, \\
b_8 &= \frac{(1+\epsilon_1)(1+\epsilon_2)(2\epsilon_4 - 2\epsilon_3 - \epsilon_5)}{8}, \\
b_{10} &= -\frac{(1-\epsilon_1)(1+\epsilon_2)(2\epsilon_4 - \epsilon_5)}{8}.
\end{aligned}
\tag{16}
$$

These equations can be inverted to solve for the errors in terms of the Fourier coefficients. The equations for a_0 and a_{10} yield

$$
\epsilon_1 = 3 - 8(a_0 + a_{10}), \qquad \epsilon_2 = \frac{4(a_0 - a_{10}) - 1}{1 - 4(a_0 - a_{10})}. \tag{17}
$$

The equations for a_8 and a_{10} also yield ϵ_1 and ϵ_2:

$$
\epsilon_1 = \frac{(a_8 - a_{10})}{(a_8 - a_{10})}, \qquad \epsilon_2 = 8(a_8 + a_{10}) - 1. \tag{18}
$$

The addition of the equations for b_4 and b_6 gives

$$
\epsilon_3 = -2(b_4 + b_6). \tag{19}
$$

The equation for b_2 can now be used to obtain

$$
\epsilon_5 = \frac{8b_2}{(1+\epsilon_1)(1-\epsilon_2)} + 2\epsilon_3, \tag{20}
$$

and finally taking the difference between b_4 and b_6 results in

$$\epsilon_4 = \epsilon_5 + 2(b_4 - b_6). \tag{21}$$

These values for the errors are now to be substituted back into the equations for the Mueller matrix elements given in Eq. (11) of Goldstein and Chipman[18] by using measured values of the Fourier coefficients.

5. Optical Properties from the Mueller Matrix

One objective of this study is to obtain electro- and magneto-optic coefficients of crystals. The coefficients are derived from Mueller matrices measured as a function of applied field strength. The method by which this derivation is accomplished is described in Goldstein *et al.*[19] and is briefly summarized here.

The application of an electric field across a crystal produces an index change. Principal indices are obtained by solving an eigenvalue problem. For example, for a $\bar{4}3m$ cubic material with index n_o and with a field E perpendicular to the (110) plane, the index ellipsoid is

$$\frac{x^2 + y^2 + z^2}{{n_o}^2} + \sqrt{2} r_{41} E(yz + zx) = 1. \tag{22}$$

The eigenvalue problem is solved, and the roots of the secular equation are the new principal indices:

$$\begin{aligned} n_x' &= n_o + \tfrac{1}{2} {n_o}^3 r_{41} E, \\ n_y' &= n_o - \tfrac{1}{2} {n_o}^3 r_{41} E, \\ n_z' &= n_o. \end{aligned} \tag{23}$$

The principal indices of the $\bar{4}3m$ cubic material for an electric field applied transversely and longitudinally are given by Namba.[20]

field and propagation direction are both along the z axis. The refractive indices experienced by the light are in the plane containing the x and y principal axes. If the light polarization and crystal are aligned so that the polarization is 45° from either principal axis, the phase retardation will be

$$\Gamma = 2\pi(n_y' - n_x')L/\lambda, \tag{25}$$

where n_y', n_x' are the (new) principal indices with the field applied. (For crystals with natural birefringence and with no electric field, these indices may just be the principal indices.)

The phase delays for light polarized at 45° to the principal axes of the $\bar{4}3m$ material can now be calculated. The phase retardation for $\bar{4}3m$ cubic material is

$$\Gamma_{\text{cubic}} = 2\pi {n_o}^3 r_{41} EL/\lambda. \tag{26}$$

If the electric field is expressed in terms of electric potential and charge separation, i.e., $E = V/d$, then the phase retardation is

$$\Gamma_{\text{cubic}}^{\text{long}} = 2\pi {n_o}^3 r_{41} V/\lambda, \tag{27}$$

because the charge separation d is equal to the optical path through the crystal L.

The phase retardation for $\bar{4}3m$ cubic material in the transverse mode is also given by Eq. (26). In the transverse mode the charge separation is not the same as the optical path so that when E is given as V/d, the phase delay is given as

$$\Gamma_{\text{cubic}}^{\text{trans}} = 2\pi {n_o}^3 r_{41} VL/d\lambda. \tag{28}$$

The cubic crystal described is expected to act as a linear retarder. The Mueller matrix formalism representation of a retarder with a fast axis at arbitrary orientation angle θ is

$$\begin{bmatrix} 1 & 0 & 0 & 0 \\ 0 & \cos^2 2\theta + \sin^2 2\theta \cos\delta & (1 - \cos\delta)\sin 2\theta \cos 2\theta & -\sin 2\theta \sin\delta \\ 0 & (1 - \cos\delta)\sin 2\theta \cos 2\theta & \sin^2 2\theta + \cos^2 2\theta \cos\delta & \cos 2\theta \sin\delta \\ 0 & \sin 2\theta \sin\delta & -\cos 2\theta \sin\delta & \cos\delta \end{bmatrix}, \tag{29}$$

The phase retardation accumulated by polarized light in traversing a medium with anisotropic properties is given by

$$\Gamma = 2\pi(n_a - n_b)L/\lambda, \tag{24}$$

where L is the medium thickness in the direction of propagation, λ is the wavelength of light, and n_a, n_b are the indices experienced in two orthogonal directions perpendicular to the direction of propagation. In the longitudinal mode of operation, the electric

where the retardance is δ. If the retarder fast axis is assumed to be at 0°, the matrix becomes, substituting for δ the retardance of the crystal,

$$\begin{bmatrix} 1 & 0 & 0 & 0 \\ 0 & 1 & 0 & 0 \\ 0 & 0 & \cos\dfrac{2\pi}{\lambda} n^3 r_{41} V \dfrac{L}{d} & \sin\dfrac{2\pi}{\lambda} n^3 r_{41} V \dfrac{L}{d} \\ 0 & 0 & -\sin\dfrac{2\pi}{\lambda} n^3 r_{41} V \dfrac{L}{d} & \cos\dfrac{2\pi}{\lambda} n^3 r_{41} V \dfrac{L}{d} \end{bmatrix}. \tag{30}$$

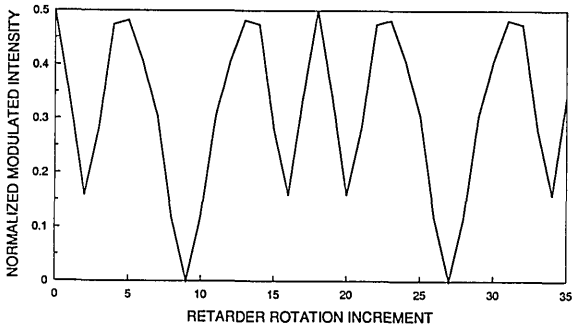

Fig. 5. Modulated intensity with no sample in the polarimeter. The first retarder is oriented at $(n-1)\times 5°$, $n = 0, 1, \ldots 35$. The second retarder is oriented at $(n-1)\times 25°$. The Mueller matrix is determined from the Fourier coefficients of this signal.

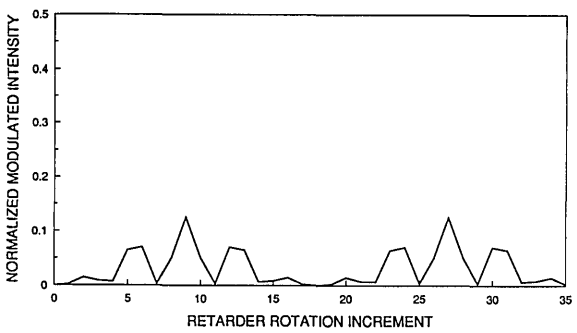

Fig. 7. Modulated intensity with vertical linear polarizer as the polarimeter sample.

It is now clear that the electro-optic coefficient r_{41} can be obtained from the measured Mueller matrix.

Note that for purposes of obtaining the electro-optic coefficient experimentally, the fast axis of an electro-optic crystal acting as an ideal retarder can be at any orientation. The (4,4) matrix element of the matrix for a retarder with the fast axis at angle θ is independent of fast-axis orientation, and the fast-axis orientation can be eliminated elsewhere by adding the (2,2) and (3,3) matrix elements or squaring and adding elements in the fourth row and column. Given a measured Mueller matrix of a crystal, a known applied voltage, and a known refractive index, one can easily obtain the electro-optic coefficient r_{41}.

6. Measurements

Extensive measurements on commercial polarization elements and electro-optic crystals have been made with the polarimeter; however, this paper is intended as a complete description of the polarimeter, not as a report on the measurements themselves. Thus the experimental matrix results presented here show an example of a measured Mueller matrix without detailed analyses of the data. Techniques for further processing of the measured Mueller matrices, e.g., to eliminate nonphysical noise, are beyond the scope of this paper.

Simulated polarimeter intensity patterns are shown in Figs. 5–8 for several ideal polarization elements. Experimental results were obtained for the corresponding real polarizers and retarders but are not reproduced because the difference from the theoretical results is only enough to widen the plotted line at some parts of the curve.

Ideal and measured Mueller matrices for a calibration (no sample) are, respectively,

$$\begin{bmatrix} 1 & 0 & 0 & 0 \\ 0 & 1 & 0 & 0 \\ 0 & 0 & 1 & 0 \\ 0 & 0 & 0 & 1 \end{bmatrix},$$

$$\begin{bmatrix} 0.998 & 0.026 & 0.019 & -0.002 \\ 0.002 & 0.976 & -0.030 & 0.009 \\ 0.007 & 0.033 & 0.966 & -0.002 \\ 0.002 & -0.004 & -0.002 & 1.000 \end{bmatrix}.$$

The measured results, normalized to unity, are given without any error compensation. The measured matrix is clearly recognizable as a noisy representation of the corresponding ideal matrix. The repeatability of the measurements is very good, with variations in consecutive measurements typically of 1 part in 1000 in the nonzero Mueller matrix elements.

Error compensation may be demonstrated with the

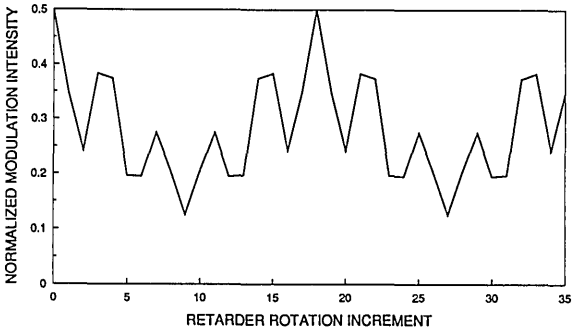

Fig. 6. Modulated intensity with horizontal linear polarizer as the polarimeter sample.

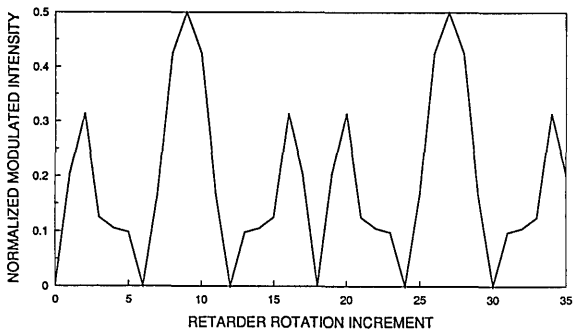

Fig. 8. Modulated intensity with half-wave plate and the fast axis at 45° as the polarimeter sample.

experimental calibration Mueller matrix. The source of the large error for the two middle elements of the diagonal is the retardance errors of the wave plates. Using calculated values for the errors and compensating by using the small-angle-approximation error analysis as discussed above and in Ref. 18, one sees that the renormalized compensated Mueller matrix for no sample becomes

$$\begin{bmatrix} 0.997 & -0.006 & 0.004 & 0.002 \\ 0.007 & 1.000 & -0.007 & 0.009 \\ 0.008 & -0.007 & 0.990 & -0.003 \\ 0.003 & -0.006 & -0.007 & 0.998 \end{bmatrix}.$$

Equations for an exact error compensation have been derived[21] for an infrared spectropolarimeter[22] and give slightly better results.

7. Conclusions

An infrared laser polarimeter has been constructed to measure the Mueller matrix of material samples in transmission. The instrument is ideally suited for calibrating infrared polarization elements. It is also intended for studies of induced birefringence resulting from the application of electric or magnetic fields. Fundamental constants of materials, such as the linear or nonlinear electro-optic tensor coefficients and the Verdet constant, can then be obtained from measurements of the Mueller matrix as a function of applied field strength. Because the complete Mueller matrix is obtained, the full characterization of electro- or magneto-optic materials that might be expected to produce scattering and depolarization, such as liquid crystals or microcrystalline materials, is also possible.

This polarimeter has been designed to fulfill the specific need of an instrument that measures polarization and fundamental electro- and magneto-optic properties of transmissive bulk materials in the infrared. It has an advantage over other polarimeters and ellipsometers in that it measures the entire Mueller matrix, makes these measurements in the infrared, and is designed to compensate, with novel hardware features and data-reduction techniques, for the major error sources (beam wander, nonideal retarders, and element-orientation misalignments). The polarimeter has been an effective tool in accurately characterizing polarization elements. Future papers will present polarimeter measurements of optical elements and fundamental properties of specific electrooptical materials.

This research was supported by the U.S. Air Force Office of Scientific Research.

References

1. R. M. A. Azzam and N. M. Bashara, *Ellipsometry and Polarized Light,* 1st ed. (North-Holland, Amsterdam, 1977), Chap. 3, p. 155.
2. D. H. Goldstein, "Applications and limitations of polarimetry," in *Polarimetry: Radar, Infrared, Visible, Ultraviolet, and X-Ray,* R. A. Chipman and J. W. Morris, eds., Proc. Soc. Photo-Opt. Instrum. Eng. **1317,** 210–222 (1990).
3. C. H. Ma, D. P. Hutchinson, P. A. Staats, and K. L. Vander Sluis, "FIR interferometer/polarimeter system on ISX-B tokamak," Rev. Sci. Instrum. **56,** 911–913 (1985).
4. E. S. Yeung, "Laser-based polarimetry enhances biochemical detection," Laser Focus/Electro-Optics **21**(2), 30–40 (1985).
5. O. Brevet-Philibert, R. Brunetton, and J. Monin, "Measuring the Verdet constant: a simple, high precision, automatic device," J. Phys. E. **21,** 647–649 (1988).
6. A. Gedanken and M. Tamir, "Multiphoton optical rotary dispersion," Rev. Sci. Instrum. **58,** 950–952 (1987).
7. J. W. Wagner, J. B. Deaton, Jr., and E. M. Hackett, "Laser polarimeter for measuring angular displacement of bend bars," Exp. Mech. **28,** 45–49 (1988).
8. R. Lipeles and D. Kivelson, "Experimental studies of acoustically induced birefringence," J. Chem. Phys. **72,** 6199–6208 (1980).
9. R. C. Thompson, J. R. Bottiger, and E. S. Fry, "Measurement of polarized light interactions via the Mueller matrix," Appl. Opt. **19,** 1323–1332 (1980).
10. R. M. A. Azzam, "Photopolarimetric measurement of the Mueller matrix by Fourier analysis of a single detected signal," Opt. Lett. **2,** 148–150 (1978).
11. P. S. Hauge, "Mueller matrix ellipsometry with imperfect compensators," J. Opt. Soc. Am. **68,** 1519–1528 (1978).
12. H. B. klein Brink, "Birefringence of the human crystalline lens *in vivo,*" J. Opt. Soc. Am. A **8,** 1788–1793 (1991).
13. H. B. klein Brink and G. J. van Blokland, "Birefringence of the human foveal area assessed *in vivo* with Mueller-matrix ellipsometry," J. Opt. Soc. Am. A **5,** 49–57 (1988).
14. G. J. van Blokland, "Ellipsometry of the human retina *in vivo:* preservation of polarization," J. Opt. Soc. Am. A **2,** 72–75 (1985).
15. P. S. Theocaris and E. E. Gdoutos, *Matrix Theory of Photoelasticity* (Springer-Verlag, Berlin, 1979), Chap. 4, p. 60, 64.
16. W. Shurcliff, *Polarized Light* (Oxford U. Press, London, 1962), App. 2, pp. 166–170.
17. G. Strang, *Linear Algebra and Its Applications,* 2nd ed. (Academic, New York, 1976), Chap. 3, p. 112.
18. D. H. Goldstein and R. A. Chipman, "Error analysis of a Mueller matrix polarimeter," J. Opt. Soc. Am. A **7,** 693–700 (1990).
19. D. H. Goldstein, R. A. Chipman, D. B. Chenault, and R. R. Hodgson, "Infrared material properties measurements with polarimetry and in *Electro-Optical Materials for Switches, Coatings, Sensor Optics, and Detectors,* R. Hartmann, M. J. Soileau, and V. K. Varadan, eds., Proc. Soc. Photo-Opt. Instrum. Eng. **1307,** 448–462 (1990).
20. C. S. Namba, "Electro-optical effect of zincblende," J. Opt. Soc. Am. **51,** 76–79 (1961).
21. D. B. Chenault, University of Alabama at Huntsville, Huntsville, Ala. 35899 (personal communication).
22. D. H. Goldstein and R. A. Chipman, "Infrared spectropolarimeter," U.S. patent 5,045,701 (3 September 1991).